Pulse propagation in adiabatically coupled photonic crystal coupled cavity waveguides

P. Sanchis, J. García, A. Martínez, and J. Martí

Citation: Journal of Applied Physics **97**, 013101 (2005); doi: 10.1063/1.1827345
View online: http://dx.doi.org/10.1063/1.1827345
View Table of Contents: http://scitation.aip.org/content/aip/journal/jap/97/1?ver=pdfcov
Published by the AIP Publishing

Pulse propagation in adiabatically coupled photonic crystal coupled cavity waveguides

P. Sanchis,[a] J. García, A. Martínez, and J. Martí
Valencia Nanophotonics Technology Center, Universidad Politécnica de Valencia, Camino de Vera s/n, 46022 Valencia, Spain

(Received 6 July 2004; accepted 4 October 2004; published online 13 December 2004)

A rigorous analysis of pulse propagation in planar photonic crystal (PhC) coupled cavity waveguides (CCWs) of finite length is reported. Conventional PhC waveguides, formed by a single line defect, are used at both interfaces of the CCW. An adiabatic taper based on progressively varying the radii of the spacing defects between cavities is used to achieve flat transmission bands with respect to the butt coupling case. The influence on the main parameters of the propagated pulse such as group delay, full width at half maximum and pulse attenuation are investigated for both the adiabatic and butt coupling cases. Furthermore, the Fabry-Perot formula has been used for modeling the pulse propagation along the CCW of finite length, which permits to analyze a large range of parameters avoiding the huge computation time requirements of finite-difference time-domain simulations. © *2005 American Institute of Physics*. [DOI: 10.1063/1.1827345]

I. INTRODUCTION

Photonic crystals (PhCs) are expected to be attractive candidates for the development of microscale photonic integrated circuits. Although full control of light propagation is only achieved by means of three-dimensional (3D) PhCs, two-dimensional (2D) planar PhCs, also known as PhC slabs, have been proposed to reduce fabrication complexity and take advantage of the mature semiconductor technologies.[1,2] In a PhC slab, light is confined in the direction perpendicular to the crystal plane by means of total internal reflection. On the other hand, waveguides in PhCs are usually created by forming line defects into the otherwise periodic structure.[3] However, a different approach of realizing a PhC waveguide based on introducing a chain of strongly confined point defects or cavities embedded in the PhC, known as coupled cavity waveguide (CCW) or coupled-resonator optical waveguide (CROW), has also been proposed.[4,5] Light propagation in CCWs can be explained as photon hopping between nearby cavities as a result of the overlapping of the tightly confined modes.[6] One of the main features of the CCWs regarding conventional PhC waveguides is a smaller group velocity which could give rise to the enhancement of group delay, nonlinear effects, and stimulated emission.[7]

Efficient coupling into conventional line-defect PhC waveguides has been widely investigated in the last years. However, only a few works have been focused on CCWs.[8–12] An inefficient coupling originates a number of undesired resonance peaks in the transmission spectrum which coincides with the number of cavities that form the CCW. The peak-to-valley ratio of the resonant peaks is mainly determined by the coupling efficiency at the two ends of the CCW. Therefore, flat transmission bands and high coupling efficiency may be achieved by properly controlling the CCW interfaces, thus avoiding the abrupt change in reflectivity.[13]

Efficient coupling into CCWs can be a critical point to avoid the distortion of ultrashort pulses propagated through CCWs of finite length. Pulse propagation has been analyzed by means of simulations and experiments in bulk PhC,[14,15] line-defect PhC waveguides,[16,17] as well as in CCWs.[8,18,19] In almost all the works, pulse propagation has been analyzed in order to study the dispersion features of PhCs. However, only the work of Lan *et al.*[8] is focused on the analysis of pulse propagation from the coupling point of view. In this paper, the dynamic performance of an adiabatic coupling technique between single-line-defect waveguides (SLWGs) and CCWs in 2D PhCs is analyzed. The proposed coupling technique is based on varying progressively the radii of the spacing defects between cavities in order to gradually match the SLWG and CCW modes.[11] A rigorous analysis of pulse propagation in both frequency and time domains is carried out in order to analyze the influence of coupling efficiency on the main parameters of the propagated pulse. The obtained results from the proposed adiabatic coupling technique are compared with the case of butt coupling between the SLWGs and the CCW of finite length. Thereby, a comprehensive explanation of the origin of the pulse degradation when the CCW is inefficiently coupled is provided. We show that pulse degradation is simply originated due to the overlapping between the transmitted pulse and the reflected pulses produced due to the high reflection at the CCW interfaces. Furthermore, the Fabry-Perot formula has been used to study a large variety of parameters dramatically reducing the computation time with respect to finite-difference time-domain FDTD simulations.

II. THEORETICAL MODEL

The PhC structures here analyzed are depicted in Fig. 1. The PhC is formed by a two-dimensional triangular lattice of dielectric rods of silicon (Si) surrounded by a homogeneous dielectric medium of silica (SiO_2). The radius of the rods is $R=0.2a$, where a is the lattice constant. All the parameters

[a]Electronic mail: pabsanki@ntc.upv.es

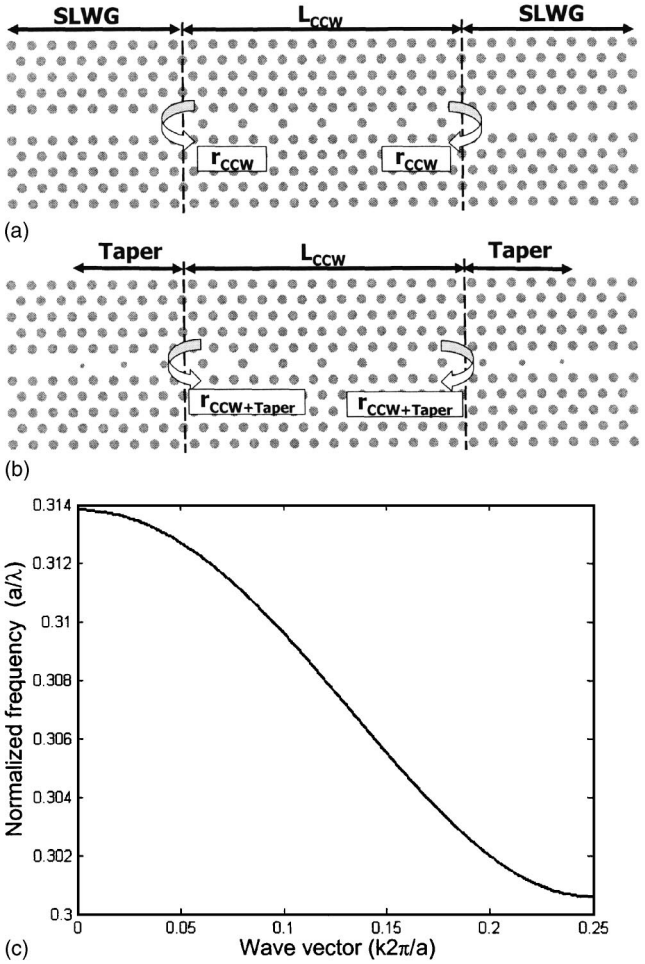

FIG. 1. Schematic representation of the analyzed structures. A coupled cavity waveguide (CCW) of finite length is (a) butt coupled and (b) adiabatically coupled to single line defect waveguides (SLWGs). (c) Dispersion relation of the CCW for the parameters considered.

are the same that in our previous work.[11] We also want to point out that a similar PhC structure to the one proposed here was recently fabricated.[20] A SLWG is used to couple light into and out a CCW of finite length. Both waveguides are created along the ΓK direction. The CCW consists of neighboring cavities formed by removing individual rods and the spacing between cavities is of one rod. Figure 1(a) shows the butt coupled CCW while Fig. 1(b) shows the adiabatically coupled CCW. The well-known Fabry-Perot formula has been used for modeling the pulse propagation along the CCW of finite length.[21] The transmission response in amplitude can be written as

$$t_{FP}(f_n) = \frac{-t^2 \exp\left(-j\frac{2\pi}{a}kL\right)}{1 - r^2 \exp\left(-j\frac{4\pi}{a}kL\right)}, \tag{1}$$

where f_n is the normalized frequency, k is the normalized wave vector, L is the cavity length, and t and r are the amplitude transmission and reflection coefficients. The relation between f_n and k is determined by the dispersion diagram, which is shown in Fig. 1(c), which was calculated by means of the plane-wave expansion method.[22] The reflection coefficients for the butt coupled and the adiabatically coupled CCW, depicted in Fig. 1, were calculated with a semianalytic method similar to that proposed in Ref. 23. The details of the method will be published elsewhere. The power reflection R as a function of the normalized frequency is shown in Fig. 2 for both structures. The adiabatic taper considered is formed by nine intermediate rods with a linear variation of their radius.[11] It can be seen that the reflection is almost negligible for a broad frequency range in agreement with the results reported in Ref. 11.

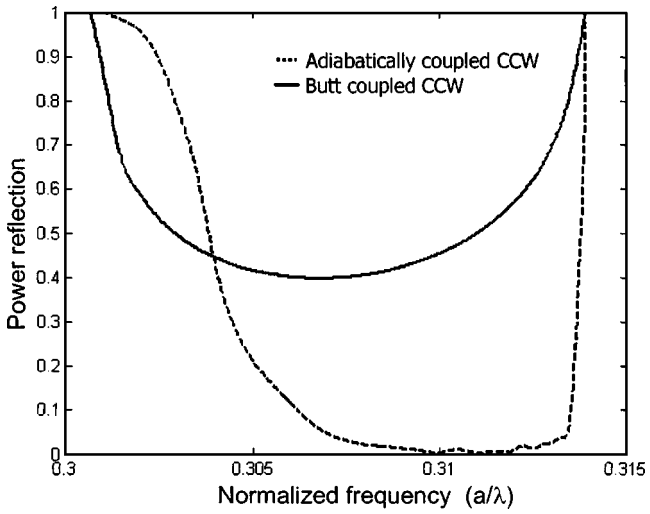

FIG. 2. Power reflection as a function of the normalized frequency.

The amplitude reflection is calculated as

$$r = \sqrt{R} \tag{2}$$

and the amplitude transmission is obtained from Eq. (2) as

$$t = \sqrt{1 - r^2} \tag{3}$$

because radiation modes are not allowed in the PhC and both the CCW and the SLWG are single mode. The power transmission spectrum is calculated as

$$T_{FP}(f_n) = |t_{FP}(f_n)|^2. \tag{4}$$

Figures 3 and 4 show the transmission spectra calculated with Eq. (4) (dashed line) and the transmission spectra calculated by using a FDTD code (solid line) for the butt coupled and the adiabatically coupled CCW respectively.[24] The CCW has a length of $L=16a$ in both cases. A very good agreement can be seen between the Fabry-Perot model and FDTD simulation for the butt coupled CCW shown in Fig. 3. The amplitude of the resonance peaks, principally at the band edges, is lower in the FDTD simulation because a higher frequency resolution requires a very short time step, which will significantly increase the simulation time. On the other hand, the number of resonances in the adiabatically coupled CCW, shown in Fig. 4, is higher in the FDTD spectrum compared to the theoretical results. This is because the total cavity length will not only depend on the CCW length but also on the input and output tapers length. However, the taper sections can not be modelled by using the Fabry-Perot model since the dispersion relation is also modified along the

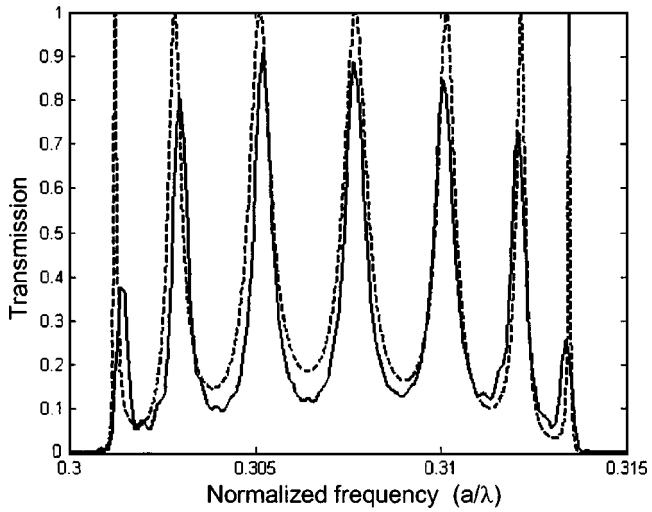

FIG. 3. Transmission spectra calculated with the Fabry-Perot formula (dashed line) and with a finite-difference time-domain code (solid line) for the butt coupled CCW.

taper.[11] But, we are mainly interested in the range of frequencies of flat transmission in which the Fabry-Perot model and FDTD simulations agree quite well. Even in this case, it is important to notice that the tapered sections may introduce an additional broadening and group delay on the propagated pulse which is not taken into account by the Fabry-Perot model. However, the broadening is usually negligible due to the short length of the taper while the group delay can be theoretically estimated, as it will be shown later.

The main advantage of using the theoretical model is that the computational time is significantly reduced compared to the FDTD simulations. Therefore, a large variety of parameters can be easily analyzed. The procedure is the following. A Gaussian source is used as input pulse. The input pulse is Fourier transformed and multiplied by the Fourier transform of Eq. (1). Thereby, the spectrum response of the output pulse is obtained and the time response is calculated by the inverse Fourier transform. The main parameters of the input pulse that can be adjusted are the full width at half maximum (FWHM) and the central frequency while the amplitude is normalized.

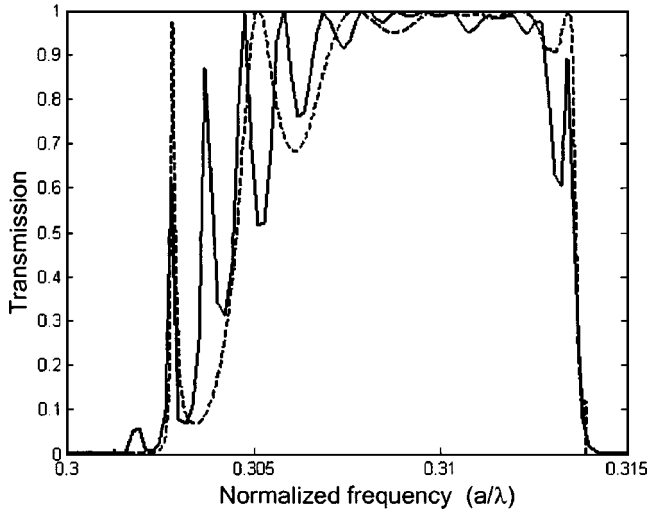

FIG. 4. Transmission spectra calculated with the Fabry-Perot formula (dashed line) and with a finite-difference time-domain code (solid line) for the adiabatically coupled CCW.

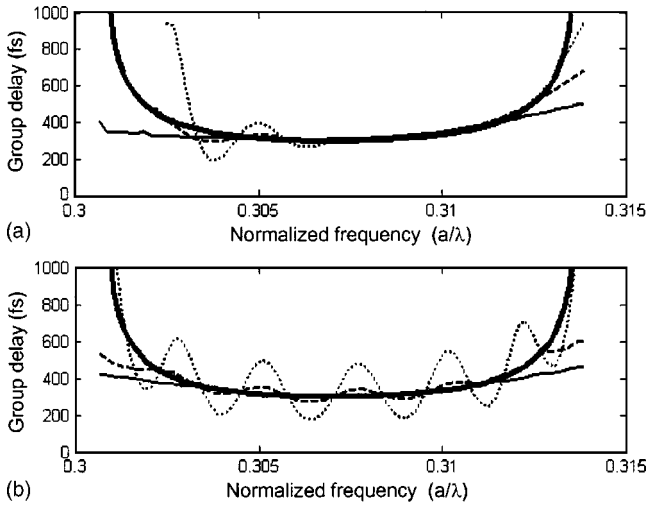

FIG. 5. Group delay of the output pulse as a function of the normalized central frequency of the input pulse for (a) the adiabatically and (b) butt coupled CCW of length $L=16a$. The solid, dashed, and dotted lines show the results for a FWHM of the input pulse of 250, 500, and 1000 fs, respectively. The thicker solid line shows the theoretical group delay calculated from the dispersion relation of the CCW.

III. RESULTS AND DISCUSSION

A. Frequency domain analysis

Figures 5–7 show the group delay, FWHM and peak amplitude of a pulse propagated through the CCW of finite length ($L=16a$) as a function of the central frequency of the input pulse. Results were obtained by using the Fabry-Perot model. Three input pulses of different FWHM have been considered: 250, 500, and 1000 femtosecond (fs). In this case, a lattice constant of 465 nm was considered. First of all, it can be seen that the group delay when the input pulse

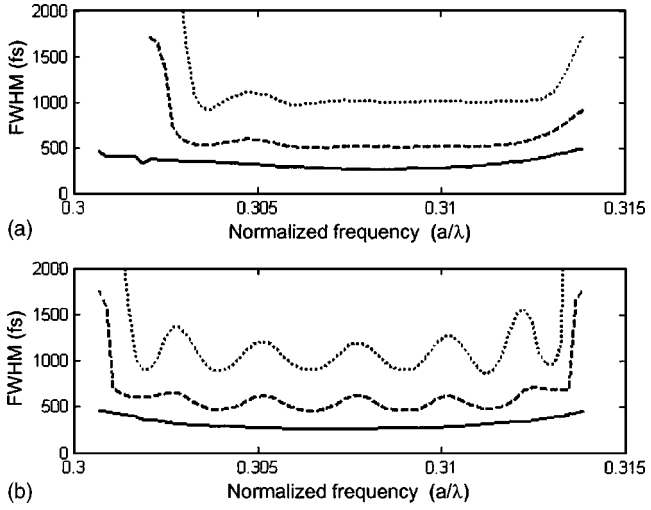

FIG. 6. Full width at half maximum (FWHM) of the output pulse as a function of the normalized central frequency of the input pulse for (a) the adiabatically and (b) butt coupled CCW of length $L=16a$. The solid, dashed, and dotted lines show the results for a FWHM of the input pulse of 250, 500, and 1000 fs, respectively.

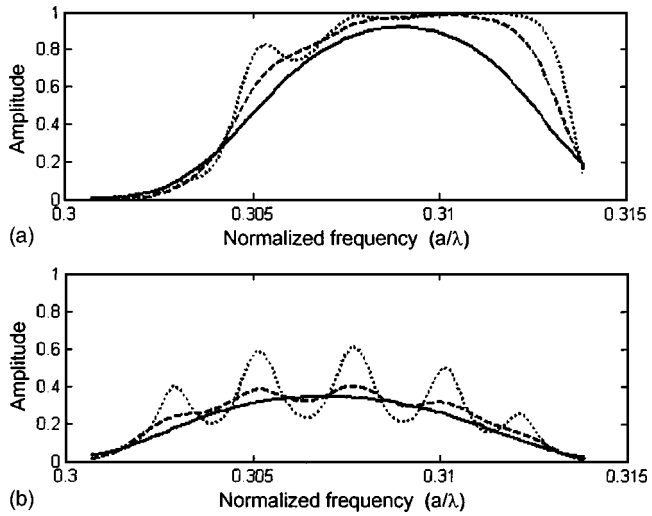

FIG. 7. Peak amplitude of the output pulse as a function of the normalized central frequency of the input pulse for (a) the adiabatically and (b) butt coupled CCW of length $L=16a$. The solid, dashed, and dotted lines show the results for a FWHM of the input pulse of 250, 500, and 1000 fs, respectively.

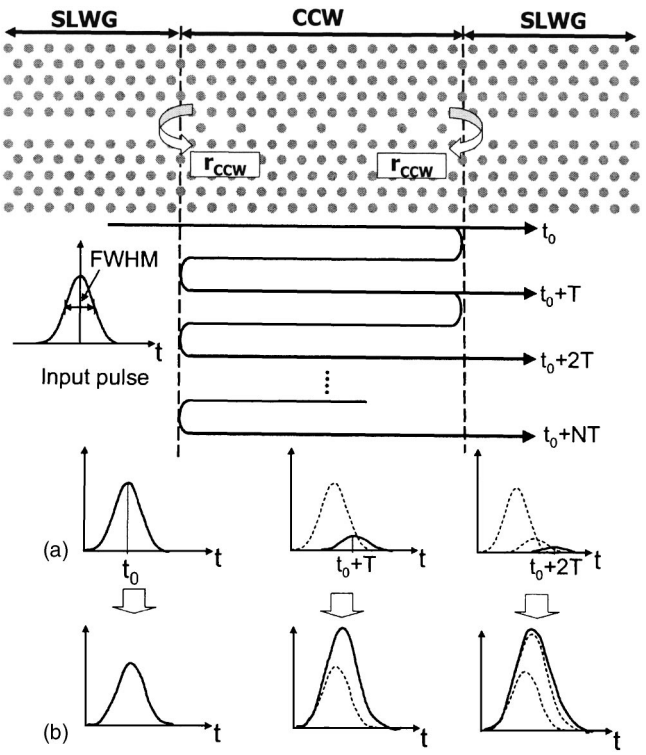

FIG. 8. Effect of the overlapping between pulses due to the inefficient coupling at the CCW interfaces. (a) The transmitted pulse t_0 and successive reflected pulses t_0+NT which are transmitted out of the CCW after they travel back and forth along the CCW, interfere among them forming the total transmitted pulse. (b) The output pulse evolution in time after each reflected pulse is transmitted out the CCW. The pulses in dashed line represent the pulses of previous step times. T is the round-trip delay, which depends on the CCW length and the group velocity given for the central frequency of the input pulse. In this example, the input pulse has a FWHM of 1000 fs and central frequency of $0.3101(a/\lambda)$ while the CCW length is $16a$.

is propagated through the adiabatically coupled CCW, shown in Fig. 5(a), is practically the same for the three widths of the input pulse. The thicker solid line shows the theoretical group delay calculated from the dispersion relation of the CCW, depicted in Fig. 1(b), and particularized for the CCW length considered ($L=16a$). A very good agreement is seen with results obtained by using the Fabry-Perot model. The increase of group delay at the band edges is due to the low group velocity of the guided mode at those frequencies. On the other hand, the group delay oscillates with frequency when the input pulse is propagated through the butt coupled CCW, as can be seen in Fig. 5(b). The origin of this oscillation, which can also be seen as an oscillation of the group velocity, is consequence of the overlapping between the transmitted pulse and the successive reflected pulses, which are transmitted out of the CCW after they travel a number of times back and forth along the CCW depending on the reflection at the interfaces. Figure 8 explains more clearly this effect. The increase or decrease of group delay with respect to the ideal case depends on the constructive or destructive interference between the transmitted and reflected pulses, which depends on the CCW length and the central frequency of the input pulse, but also on the width of the input pulse, as it will be explained more in detail later. Therefore, the group delay in the adiabatically coupled CCW, shown in Fig. 5(a), begins to oscillate at the low frequencies of the band due to the increase of reflection that occurs at those frequencies. Furthermore, it can be seen that oscillations of group delay have higher amplitude as the FWHM of the input pulse increases in both the butt coupled and adiabatically coupled CCW. For the narrower input pulse, the overlapping will be almost negligible and hence the group delay responses in both structures will be the same. The effect of the overlapping between successive pulses can be estimated by comparing the FWHM and the round trip delay, which is defined as $2L/v_g$ where L is the CCW length and v_g is the group velocity. For the particular case of $L=16a$ (7.44 μm) and a central frequency of the input pulse of $0.3101(a/\lambda)$ that corresponds to a $v_g \sim 0.02$ fs/μm, the round trip delay is 744 fs. When the FWHM is much lower than the round trip delay, the overlapping will be almost negligible. Therefore, the group delay responses for the input pulse with FWHM=250 fs, shown with solid lines in Fig. 5, are not affected independently of the reflection at the CCW interfaces. However, it is important to point out that the amplitude of the output pulse is still affected by the transmission efficiency at the CCW interfaces. Furthermore, a train of successive pulses appears at the output of the CCW when high reflection exists at the interfaces.

The same behavior than that of the group delay response can be observed for the FWHM and peak amplitude of the output pulse, as shown in Figs. 6 and 7. The FWHM is similar as that of the input pulse, as shown Fig. 6(a), when the reflection at the CCW interfaces is negligible, but it starts to oscillate with frequency, as shown in Fig. 6(b), when the reflection grows up. The increase of the FWHM at the band edges is due to the larger group velocity dispersion (GVD). Furthermore, when narrower input pulses are considered, the FWHM of the output pulse at frequencies located in the middle of the band is slightly higher than that of the input pulse because of the pulse spectral width covers a higher bandwidth increasing the effect of GVD. On the other hand,

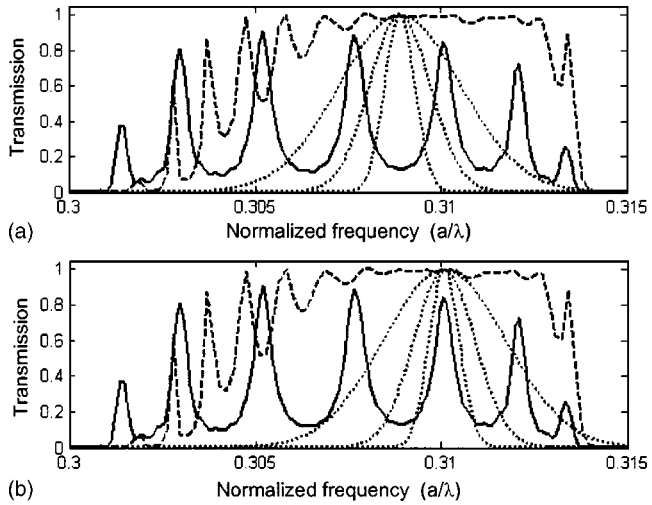

FIG. 9. Transmission spectra of the input pulse for a normalized central frequency of (a) $0.3089(a/\lambda)$ and (b) $0.3101(a/\lambda)$. The FWHM of the input pulse is 250 (broader spectrum), 500, and 1000 fs (narrower spectrum). The solid and dashed lines show the transmission spectra of the butt coupled and adiabatically coupled CCW of length $L=16a$.

the attenuation of the output pulse is very low when the adiabatically coupled CCW is used, as it can be seen in Fig. 7(a), except at the low frequencies of the band, which is again expected due to the higher reflection shown in Fig. 2. Furthermore, there is a slight bandwidth reduction at low frequencies compared to the butt coupled CCW response,[11] shown in Fig. 7(b), which also explains the bandwidth reduction of Figs. 5(a) and 6(a). It can also be seen that, as mentioned previously, although the group delay and FWHM responses in both the butt coupled and the adiabatically coupled CCW are the same when narrower input pulses are considered due to the lower overlapping between the transmitted and reflected pulses, the attenuation of the output pulse is much higher in the butt coupled CCW than in the adiabatically coupled CCW due to the lower transmission efficiency, as shown in Fig. 7.

B. Time domain analysis

Comparing the results shown in Figs. 5(b), 6(b), and 7(b) with the transmission spectrum of the butt coupled CCW shown in Fig. 3, it can be seen that the maximums and minimums in the transmission spectrum correspond to maximums and minimums of group delay, FWHM and peak amplitude of the output pulse. This behavior derives from the fact that when the central frequency of the input pulse coincides with a maximum of the transmission spectrum, the transmitted pulse interferes constructively with the reflected pulses so the width of the output pulse is increased as well as the group delay. Furthermore, the pulse attenuation decreases because the transmission efficiency is higher. The opposite performance occurs when the central frequency of the input pulse coincides with a minimum of the transmission spectrum. In order to analyze this behavior in depth, time domain pulse propagation has been analyzed at two different normalized central frequencies of the input pulse, $0.3089(a/\lambda)$ and $0.3101(a/\lambda)$, which correspond to a minimum and a maximum of the transmission spectrum, respectively, for the butt coupled CCW. The input pulse spectra corresponding to FWHMs of 250, 500, and 1000 fs are shown in Fig. 9(a) for the central frequency of $0.3089(a/\lambda)$ and in Fig. 9(b) for the central frequency of $0.3101(a/\lambda)$. The transmission spectrum of the adiabatically coupled CCW is also shown in Fig. 9. The group delay, FWHM and amplitude of the output pulse have been obtained by means of FDTD simulations as well as with the Fabry-Perot model. Tables I and II show the results for the butt coupled CCW for the two different central frequencies considered whereas Tables III and IV show the results for the adiabatically coupled CCW. First of all, it can be seen that FDTD simulations and theoretical results agree quite well. Regarding the group delay, the excess delay introduced by the input and output SLWGs have been added to the group delay obtained from the Fabry-Perot model to better compare with FDTD simulations. This additional delay can be theoretically estimated from the dispersion relation of the SLWG. Furthermore, the input and output tapers also introduce an additional delay in the adiabatically coupled CCW, which has also been added in Tables III and IV to the group delay obtained from the Fabry-Perot model. This delay can be estimated for a particular normalized frequency with

$$\Delta\tau_{\text{taper}}(f_n)=\sum_{i=1}^{LT}4a/v_g^i(f_n), \tag{5}$$

where $4a$ is twice the length of the intermediate sections that form the taper, a being the lattice constant, $vg_i(f_n)$ is the

TABLE I. Full width at half maximum (FWHM) (fs), group delay (fs), and peak amplitude of the output pulse as a function of the FWHM of the input pulse considering the butt coupled CCW. Results of FDTD simulations and the Fabry-Perot model are compared. Regarding the group delay, the excess delay (~330 fs) introduced by the input and output SLWGs have been added to the group delay obtained from the Fabry-Perot model to better compare with FDTD simulations. The central frequency of the input pulse is $0.3089(a/\lambda)$ and the CCW length is $L=16a$.

	Fabry-Perot model			FDTD simulations		
FWHM	FWHM	Delay	Amplitude	FWHM	Delay	Amplitude
250	264.281	650.117	0.3096	258.923	672.758	0.2905
500	456.464	617.405	0.3021	449.696	635.064	0.2712
1000	897.418	513.253	0.2147	876.925	512.112	0.1827

TABLE II. Full width at half maximum (FWHM) (fs), group delay (fs), and peak amplitude of the output pulse as a function of the FWHM of the input pulse considering the butt coupled CCW. Results of FDTD simulations and the Fabry-Perot model are compared. Regarding the group delay, the excess delay (~328 fs) introduced by the input and output SLWGs have been added to the group delay obtained from the Fabry-Perot model to better compare with FDTD simulations. The central frequency of the input pulse is $0.3101(a/\lambda)$ and the CCW length is $L=16a$.

	Fabry-Perot model			FDTD simulations		
FWHM	FWHM	Delay	Amplitude	FWHM	Delay	Amplitude
250	281.295	669.549	0.2528	291.447	697.809	0.2557
500	621.622	699.535	0.3128	654.569	745.185	0.3514
1000	1266.51	873.341	0.5028	1214.06	897.606	0.5670

TABLE III. Full width at half maximum (FWHM) (fs). group delay (fs), and peak amplitude of the output pulse as a function of the FWHM of the input pulse considering the adiabatically coupled CCW. Results of the FDTD simulations and the Fabry-Perot model are compared Regarding the group delay, the excess delay (~460 fs) introduced by the input and output SLWGs and tapers have been added to the group delay obtained from the Fabry-Perot model to better compare with FDTD simulations. The central frequency of the input pulse is $0.3089(a/\lambda)$ and the CCW length is $L=16a$

	Fabry-Perot model			FDTD simulations		
FWHM	FWHM	Delay	Amplitude	FWHM	Delay	Amplitude
250	263.858	784.347	0.9193	263.200	814.886	0.9344
500	499.704	774.101	0.9698	502.195	799.799	0.9856
1000	995.46	767.521	0.9609	1000.830	797.309	0.9905

group velocity at the corresponding normalized frequency calculated from the intermediate dispersion diagrams of the taper,[11] and LT is the taper length. For instance, the additional delay for the butt coupled CCW due to the input and output SLWGs, whose total length is $51a$, at the normalized frequency of $0.3089(a/\lambda)$ will be around 330 fs, whereas the additional delay for the adiabatically coupled CCW will be around 460 fs, being 360 fs due to the input and output tapers, calculated with Eq. (5) and whose total length is $36a$ and being 100 fs due to the input and output SLWGs, whose total length is $15a$. On the other hand, the results shown in Tables I and II corroborate that the group delay, FWHM, and amplitude of the output pulse decrease with respect to the ideal performance when the central frequency of the input pulse coincides with a minimum of the transmission spectrum while they increase when the central frequency of the input pulse coincides with a maximum of the transmission spectrum. Furthermore, this effect becomes more noticeable as the input pulse is wider.

The input pulse (FWHM=1000 fs) as well as the output pulses propagated through the butt coupled CCW when the central frequency of the input pulse is $0.3101(a/\lambda)$ and $0.3089(a/\lambda)$ are shown in Figs. 10(a)–10(c), respectively. It should be noticed that only the envelope of the pulse is shown and therefore the time response of the input pulse for both central frequencies will be the same (only the time offset will be slightly different). From the results shown in Fig.

TABLE IV. Full width at half maximum (FWHM) (fs), group delay (fs), and peak amplitude of the output pulse as a function of the FWHM of the input pulse considering the adiabatically coupled CCW. Results of FDTD simulations and the Fabry-Perot model are compared. Regarding the group delay, the excess delay (~455 fs) introduced by the input and output SLWGs and tapers have been added to the group delay obtained from the Fabry-Perot model to better compare with FDTD simulations. The central frequency of the input pulse is $0.3101(a/\lambda)$ and the CCW length is $L=16a$.

	Fabry-Perot model			FDTD simulations		
FWHM	FWHM	Delay	Amplitude	FWHM	Delay	Amplitude
250	276.877	806.466	0.8843	278.005	835.848	0.8299
500	503.981	797.912	0.9816	503.464	827.071	0.9716
1000	1002.79	795.374	0.9937	1002.79	817.329	0.9807

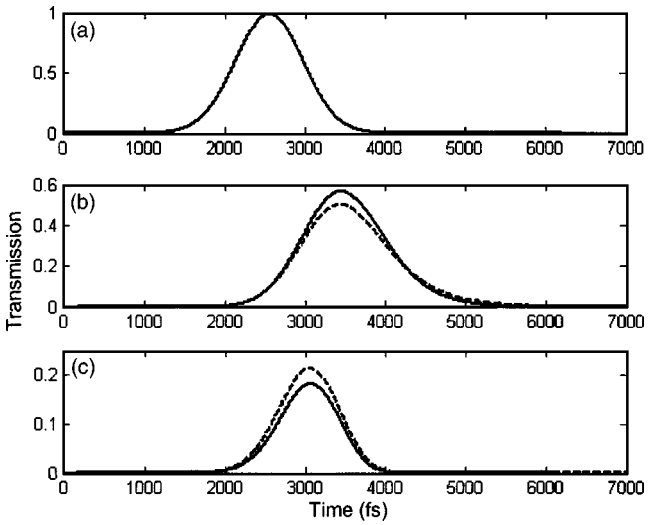

FIG. 10. Pulse propagation through the butt coupled CCW for (a) an input pulse (FWHM=1000 fs) with central frequencies, (b) $0.3101(a/\lambda)$, and (c) $0.3089(a/\lambda)$. The solid line shows FDTD simulations while the dashed line shows the results obtained with the Fabry-Perot model. The CCW length is $16a$.

10, it can be seen that an excellent agreement between FDTD results, shown with solid line, and theoretical results, shown with dashed line, is achieved. On the other hand, it can be observed that at both frequencies the rising time of the output pulse is the same than that of the input pulse. However, the falling time increases at $0.3101(a/\lambda)$, as it can be seen in Fig. 10(b), due to the constructive interference between the transmitted and reflected pulses while it decreases at $0.3089(a/\lambda)$, as it can be seen in Fig. 10(c), due to the destructive interference between the transmitted and reflected pulses. Therefore, the FWHM as well as the group delay increases in the former while decreases in the latter. Furthermore, the attenuation of the output pulse is much lower in the former than in the latter. It is important to point out that the increase or decrease of FWHM and group delay is an artificial artifact due to the overlapping between the transmitted and reflected pulse and not due to a variation of the dispersion relation associated with the finite length of the CCW.

The same behavior takes place when the input pulse has a FWHM of 500 fs, as shown in Fig. 11. However, in this case the reflected pulses, which travel several times back and forth along the CCW and therefore suffer a higher delay, do not entirely overlap with the transmitted pulse due to the lower width of the input pulse. Therefore, the variation of the FWHM and group delay of the output pulse regarding the ideal performance is diminished. The reflected pulses that suffer a higher delay are seen when the central frequency of the input pulse is $0.3089(a/\lambda)$, shown in Fig. 11(c), because the destructive interference of the reflected pulses that overlap shortens the falling time of the output pulse. This performance can be clearly observed in Fig. 12, which shows the propagated pulses when the input pulse has only a FWHM of 250 fs. In this case, the reflected pulses practically do not overlap with the transmitted pulse and therefore they can be seen at both central frequencies of the input pulse, shown in Figs. 12(b) and 12(c). Therefore, the FWHM, group delay,

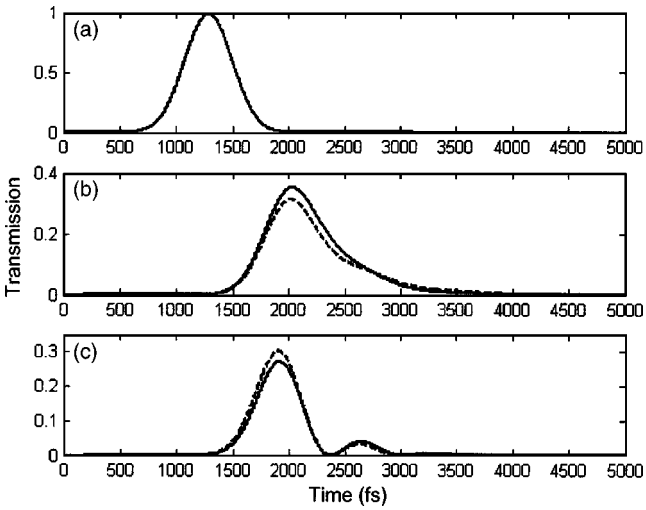

FIG. 11. Pulse propagation through the butt coupled CCW for (a) an input pulse (FWHM=500 fs) with central frequencies, (b) $0.3101(a/\lambda)$, and (c) $0.3089(a/\lambda)$. The solid line shows FDTD simulations while the dashed line shows the results obtained with the Fabry-Perot model. The CCW length is $16a$.

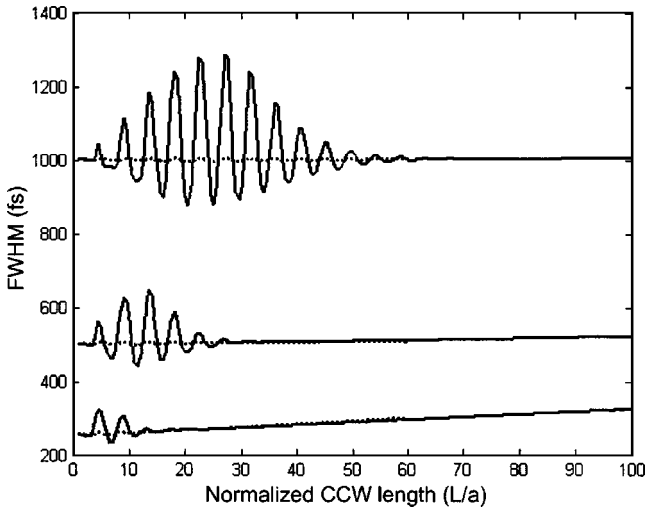

FIG. 13. FWHM of the output pulse as a function of the normalized CCW length for an input pulse of a FWHM of 250, 500, and 1000 fs and a central frequency of $0.3101(a/\lambda)$. The solid line shows the results for the butt coupled CCW while the dashed line shows the results for the adiabatically coupled CCW.

and pulse attenuation of the output pulse are similar at both frequencies. The slight differences in the FWHM and group delay are those determined due to the different behavior of the dispersion relation at both frequencies.

C. Variation of CCW length

Figure 13 shows the FWHM as a function of the normalized CCW length for the butt coupled (solid line) and the adiabatically coupled CCW (dotted line) considering that the central frequency of the input pulse is $0.3101(a/\lambda)$. Three input pulses of different FWHM have been considered: 250, 500, and 1000 fs. It can be seen that the FWHM of the output pulse does not oscillate when the adiabatic taper is used independently of the FWHM of the input pulse. On the other hand, the FWHM oscillates when the reflection into the CCW increases, i.e., for the butt coupled CCW. Furthermore, the oscillations have higher amplitude and occur in a larger range of CCW lengths when the FWHM of the input pulse increases due to the fact that the overlapping between the transmitted and reflected pulses will be larger. The highest amplitude of the oscillations arises when the round trip delay of the CCW is similar to the FWHM of the input pulse. On the other hand, the maximum or minimum of the oscillations depends on if the central frequency of the input pulse coincides or not with a maximum or minimum of the transmission spectrum. Note that the resonances in the transmission spectrum are located at different frequencies and their number decreases or increases as the CCW length becomes shorter or longer, respectively. It is also interesting to notice that if the CCW is very short, the transmitted and reflected pulses will almost entirely overlap and therefore the FWHM of the output pulse will not be affected. However, the amplitude of the output pulse will be significantly attenuated with respect to the adiabatically coupled CCW. From the results shown in Fig. 13, it can also be seen that the FWHM of the output pulse increases as the CCW is longer due to the GVD. The effect of the GVD is higher, i.e., the slope of FWHM as a function of CCW length increases, as the input pulse is narrower due to the broader spectral width.

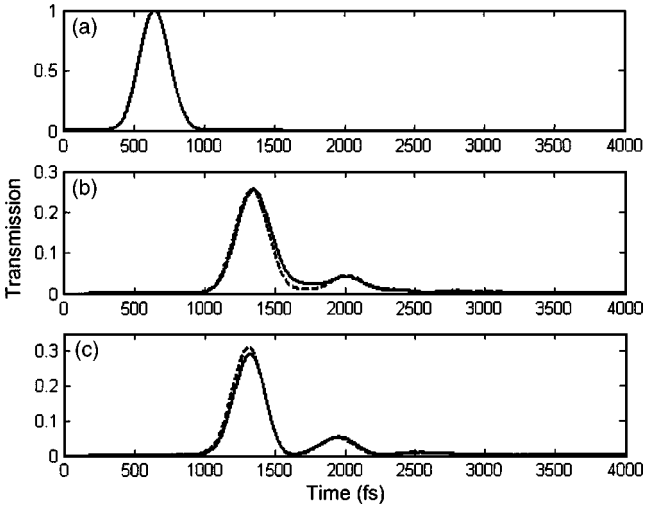

FIG. 12. Pulse propagation through the butt coupled CCW for (a) an input pulse (FWHM=250 fs) with central frequencies, (b) $0.3101(a/\lambda)$, and (c) $0.3089(a/\lambda)$. The solid line shows FDTD simulations while the dashed line shows the results obtained with the Fabry-Perot model. The CCW length is $16a$.

Figure 14 shows the group delay as a function of the normalized CCW length for the butt coupled and the adiabatically coupled CCW considering that the input pulse has a FWHM of 1000 fs and the central frequency is $0.3101(a/\lambda)$ (dashed line) and $0.3089(a/\lambda)$ (solid line). The group delay of the adiabatically coupled CCW is increased by $\Delta\tau_{taper}$, which can be estimated with Eq. (5), due to the excess of delay introduced by the input and output tapers. In Fig. 14, we have taken an arbitrary $\Delta\tau_{taper}$ in order to better interpret the results. It can be seen that the group delay in both the butt coupled and adiabatically coupled CCW increases linearly with the CCW length. However, it oscillates at shorter lengths for the former due to the overlapping between the

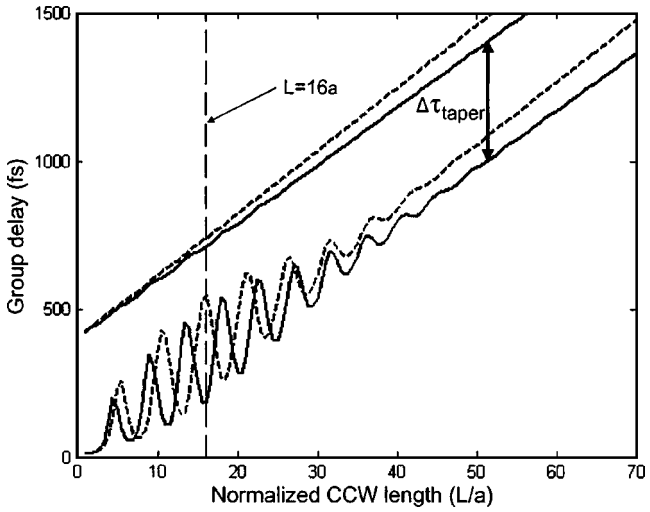

FIG. 14. Group delay of the output pulse as a function of the normalized CCW length for the butt coupled and adiabatically coupled CCW. The input pulse has a FWHM of 1000 fs and central frequencies of $0.3089(a/\lambda)$ (solid line) and $0.3101(a/\lambda)$ (dashed line).

transmitted and reflected pulses. In this case, the group delay is maximum at $0.3101(a/\lambda)$ and minimum at $0.3089(a/\lambda)$ only when the CCW length of $16a$. Obviously, this behavior does not occur for other CCW lengths because the frequency response, i.e. the number and position of resonances, is modified. On the other hand, it should be noticed that although the group delay response of both the butt coupled and the adiabatically CCW is the same for long CCWs, apart from the $\Delta\tau_{taper}$ factor, the time response of the propagated pulse will not be the same, as discussed in the previous sections. Figure 15 shows the propagated pulse as a function of time considering a CCW length of $50a$ for the butt coupled CCW [see Fig. 15(b)] and the adiabatically coupled CCW [see Fig. 15(c)]. The input pulse (FWHM=1000 fs) is shown in Fig. 15(a) and in this case $\Delta\tau_{taper}=0$. It can be seen that while the shape and group delay of the main transmitted pulse is the same in both cases, there are several additional pulses of lower amplitude in the butt coupled CCW corresponding to the successive reflected pulses. Furthermore, the output pulse is significantly attenuated for the butt coupled CCW while it is not attenuated for the adiabatically coupled CCW.

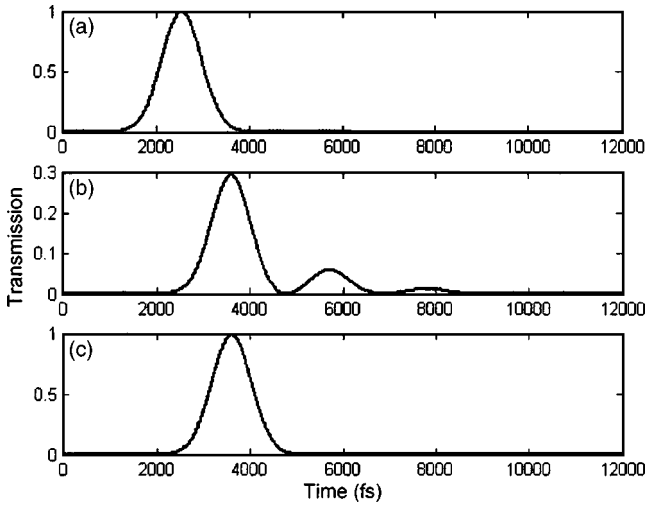

FIG. 15. (a) Input pulse of a FWHM of 1000 fs and a central frequency of $0.3101(a/\lambda)$ propagated through the (b) butt coupled and (c) adiabatically coupled CCW of a length of $50a$.

IV. CONCLUSION

The interesting features of CCWs, such as a very small group velocity, make this kind of PhC waveguide a key component for the development of compact photonic integrated devices such as optical delay lines or dispersion compensators. However, we have seen that an efficient coupling becomes mandatory in order to ensure their optimum dynamic performance. The proposed coupling technique based on progressively varying the radii of the spacing defects between cavities may to be a promising approach. On the other hand, the causes of distortion when a pulse is propagated through an inefficiently coupled CCW of finite length have been analyzed and discussed. Furthermore, a theoretical model based on the Fabry-Perot formula has been used to analyze a large variety of parameters. We want to point out that such a model could be extended for easily testing the performance of novel devices based on CCW.

ACKNOWLEDGMENTS

This work has been partially funded by the Spanish Ministry of Science and Technology under Grant No. TIC2002-01553. The authors would like to thank the Generalitat Valenciana for funding the Valencia Nanophotonics Technology Centre. P.S. acknowledges the Spanish Ministry of Education, Culture and Sport for funding his grant.

[1]T. F. Krauss, R. M. de la Rue, and S. Brand, Nature (London) **383**, 699 (1996).
[2]E. Chow *et al.*, Nature (London) **407**, 983 (2000).
[3]J. D. Joannopoulos, R. D. Meade, and J. N. Winn, *Photonic Crystals: Molding the Flow of Light* (Princeton University Press, Princeton 1995).
[4]A. Yariv, Y. Xu, R. K. Lee, and A. Scherer, Opt. Lett. **24**, 711 (1999).
[5]N. Stefanou and A. Modinos, Phys. Rev. B **57**, 12127 (1998).
[6]M. Bayindir, B. Temelkuran, and E. Ozbay, Phys. Rev. B **61**, R011 855 (2000).
[7]S. Mookherjea and A. Yariv, IEEE J. Sel. Top. Quantum Electron. **8**, 448 (2002).
[8]S. Lan, S. Nishikawa, H. Ishikawa, and O. Wada, J. Appl. Phys. **90**, 4321 (2001).
[9]M. Sumetsky and B. J. Eggleton, Opt. Express **11**, 381 (2003).
[10]T. Yang, Y. Sugimoto, S. Lan, N. Ikeda, Y. Tanaka, and K. Asakawa, J. Opt. Soc. Am. B **20**, 1922 (2003).
[11]P. Sanchis, J. Garcia, A. Martínez, F. Cuesta, A. Griol, and J. Martí, Opt. Lett. **28**, 1903 (2003).
[12]Y. H. Ye, J. Ding, D. Y. Jeong, I. C. Khoo, and Q. M. Zhang, Phys. Rev. E **69**, 056604 (2004).
[13]T. J. Karle, D. H. Brown, R. Wilson, M. Steer, and T. F. Krauss, IEEE J. Sel. Top. Quantum Electron. **8**, 909 (2002).
[14]A. Imhof, W. L. Vos, R. Sprik R, and A. Lagendijk, Phys. Rev. Lett. **83**, 2942 (1999).
[15]T. Tanaka, S. Noda, A. Chutinan, T. Asano, and N. Yamamoto, Opt. Quantum Electron. **34**, 37 (2002).
[16]S. Yamada, Y. Watanabe, Y. Katayama, and J. B. Cole, J. Appl. Phys. **93**, 1859 (2003).
[17]T. Asano, K. Kiyota, D. Kumamoto, B. S. Song, and S. Noda, Appl. Phys. Lett. **84**, 4690 (2004).
[18]S. Mookherjea and A. Yariv, Phys. Rev. E **65**, 056601 (2002).
[19]T. J. Karle, Y. J. Chai, C. N. Morgan, I. H. White, and T. F. Krauss, IEEE J. Lightwave Technol. **22**, 514 (2004).

[20]M. Tokushima, H. Yamada, and Y. Arakawa, Appl. Phys. Lett. **84**, 4298 (2004).
[21]H. A. Haus, (Prentice-Hall, Englewood Cliffs, 1984).
[22]S. G. Johnson and J. D. Joannopoulos, Opt. Express **8**, 173 (2001).
[23]P. Sanchis, P. Bienstman, B. Luyssaert, R. Baets, and J. Marti, IEEE J. Quantum Electron. **40**, 541 (2004).
[24]A. Taflove, *Computational Electrodynamics* (Artech, Norwood, MA, 1995).